Multilayered Semiconductor Membranes for Nanopore Ionic Conductance Modulation

Maria E. Gracheva,[†,§,*] Dmitriy V. Melnikov,[‡,†,§] and Jean-Pierre Leburton[‡,†,*]

[†]Beckman Institute for Advanced Science and Technology, and [‡]Department of Electrical and Computer Engineering, University of Illinois at Urbana—Champaign, Urbana, Illinois 61801. [§]Current address: Physics Department, Clarkson University.

ABSTRACT We explore the possibility of using thin layered semiconductor membranes for electrical control of the ion current flow through a nanopore, thereby operating like tunable ionic transistors. While single layer semiconductor membranes can be voltage tuned to operate as ionic filters or "switches", double layered membranes can rectify the ion current flowing through the nanopore in addition to ion filtering. Triple layer membranes exhibit enhanced functionality with characteristics similar to those of the single and double layer membranes in addition to bidirectional current blocking and switching, thereby operating similar to tunable ionic transistors.

KEYWORDS: transistor · ionic diode · doped semiconductor · surface charge · voltage-gated ion channels

The ionic selectivity of biological channels that regulate ion permeation through cell membranes is a basic mechanism of cell biology.[1,2] In recent years, the ability to create nanopores in artificial membranes has stimulated intense fundamental and applied research in attempts to replicate as well as enhance the functionality of ion channels. Hence, the properties of track-etched membranes have been studied in comparison with the properties of various biological channels,[3−5] while artificial nanopores in dielectric membranes[6,7] have been proposed as a substitute for biological ion channels.[8−10]

As a key ingredient to their functionality, the surface charge in and near the ends of biological channels can be of either signs or can even be spatially distributed in the pore.[1] Single nanopores decorated with fixed local positive charges have been proposed to operate as a "nanofluidic diode" and ion current rectifier.[11,12] Recently, conical nanopores in polymer membranes with various (negative) surface charges have been shown to act as ion rectifiers,[13−15] while a microfluidic transistor operating by modulation of surface charge in an ion channel has been proposed[16] and modeled theoretically.[17] In an artificial membrane, the presence of a surface charge is crucial for the use of nanopores for a single molecule detection, ion/protein filtering,[18] and potentially in DNA sequencing.[19−21] In general, it is very difficult to directly control or change membrane charge once it was deposited. In these designs, additional flexibility can be obtained by manipulation of the solution pH once the surface charge is deposited or *via* chemical modification of the membrane.[22] The surface charge in solid-state nanopores is usually negative and results from the fabrication process.[19]

Therefore, nanopores controlled by external bias have obvious advantages over the systems with fixed surface charge. Voltage-controlled ion selectivity of gold nanotubes was reported,[23] while gate voltage modulation of the solution concentration to change the ionic conductance was experimentally demonstrated.[24]

Advances in semiconductor technology have enabled the fabrication of nanometer-thick layers with arbitrary n- or p-doping levels;[25] recently, we showed that n-doped semiconductor membranes can attract either positive or negative ions at the nanopore surface[26] and that nanopores in the n^+-Si membrane can operate as an ion filter.[18] Furthermore, we proposed to use pn-double layer membranes as *tunable* ion filters and current rectifiers.[27]

In this paper, we predict by numerical modeling that triple layer membranes made of p- and n-type doped semiconductors, such as npn, can control the ionic current through a nanopore in a way similar to the electron current in conventional electronic transistors, with performance regimes ranging from the "ionic switch" to current blocking and rectification.

Membrane Electrostatics Model. Our Si membrane is 23 nm thick ($L = 23$ nm) (see

*Address correspondence to gracheva@clarkson.edu, jleburto@uiuc.edu.

Received for review July 24, 2008 and accepted October 21, 2008.

Published online November 6, 2008. 10.1021/nn8004679 CCC: $40.75

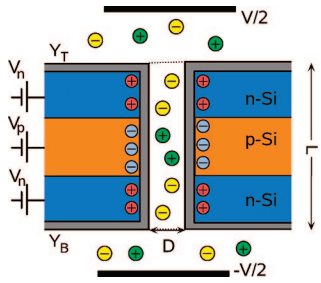

Figure 1. Geometry of the modeled nanopore in a triple layered npn-membrane.

Figure 1) and consists of three layers of n-, p-type Si with 7 nm thickness each (npn-membrane). The n-type doping is $N_d^n = 2 \times 10^{20}$ cm^{-3},[8] and is equal to the p-type doping N_d^p for all membranes. We use two nanopore designs: one has a cylindrical shape with the diameter $D = 2$ nm, while the other is a conical nanopore with constriction diameter $D = 1$ nm (in the membrane's center) and various 3−10 nm openings at the membrane surfaces. Such nanopore geometries are the results of the electron beam fabrication process.[19] The surface of the membrane is covered by a 1 nm surface layer of SiO_2 containing a fixed negative charge $\sigma = -0.0256$ C/m^2. The nanopore membrane characteristics: nanopore diameter D, membrane doping N_d,and the nanopore fixed charge σ are typical parameters known from nanopore experiments.[8,19] The membranes thickness L is chosen to fulfill two contradictory conditions: (1) the overall membrane should be as thin as possible (to speed up the separation process), and at the same time, (2) the individual membrane layers should be thick enough to avoid the depletion of charge carriers around the nanopore and at the n-type/p-type interfaces. The membrane is immersed in an electrolyte KCl solution with a concentration 0.1 M, unless otherwise noted. Each material is characterized by its relative permittivity (*i.e.*, $\varepsilon_{Si} = 11.7$, $\varepsilon_{SiO_2} = 3.9$), while the dielectric constant of the electrolyte solution is chosen $\varepsilon_{electrolyte} = 78$.

Ionic Current Model. The total ionic current through the nanopore is given by the sum of the fluxes J_i from all ion species:

$$I = F\pi r^2 \sum_i z_i J_i \qquad (1)$$

We assume that the ionic flux of individual species i, J_i, is governed by the Nernst−Planck equation:[28]

$$J_i = -D_i \frac{dc_i}{dy} - z_i D_i c_i \frac{F}{RT} \frac{d\varphi}{dy} \qquad (2)$$

where the first term describes the ion diffusion through the nanopore, while the second term is responsible for the drift of charged ions caused by the electric field $d\phi/dy$. The electrostatic potential $\phi(y)$ is the sum of the equilibrium potential $\phi^0(y)$ obtained from the solution of the Poisson equation and the potential due to the electrolyte bias V which is assumed to drop linearly across the whole membrane thickness L: $\phi(y) = \phi_0(y) - Vy/L$. In eqs 1 and 2, $F = qN_A$ is the Faraday constant ($N_A = 6.02 \times 10^{23}$ mol^{-1}), $F/RT = q/k_BT$ with the temperature $T = 300$ K (q and k_B are the elementary charge and Boltzmann constant, respectively); z_i, D_i, and c_i are the charge number ($z_i = \pm 1$ in our case), the diffusion coefficient $D_i = 2 \times 10^{-5}$cm^2/s and concentration of the ion species i, respectively; r is the nanopore radius, $2r = 2(1)$ nm for the cylindrical (conical) nanopore.

At the top Y_T (bottom Y_B) membrane interfaces ($L = Y_T - Y_B = 23$ nm; see Figure 1), the bulk c_i^0 and nanopore ion concentrations $c_i(Y_T)$ [$c_i(Y_B)$] are connected by means of the Donnan equilibrium conditions:[28,29]

$$c_i(Y_T) = c_i^0 \exp\left(-\frac{z_i F}{RT}\Delta\varphi_T^0\right) \qquad (3)$$

$$c_i(Y_B) = c_i^0 \exp\left(-\frac{z_i F}{RT}\Delta\varphi_B^0\right) \qquad (4)$$

where $\Delta\phi_T^0$ [$\Delta\phi_B^0$] is the difference between the electronstatic potential ϕ^0 in the bulk of the solution and at the membrane interface $Y_T(Y_B)$ and which is independent of the external membrane bias V.

The flux J_i is calculated from the numerical solution of the Nernst−Planck equation (eq 2) with respect to the ion concentration c_i as a fitting parameter to satisfy the boundary conditions (eqs 3 and 4).

Single Layer Membrane: Ionic Filter and Switch. In order to understand the complex behavior of the triple layered membrane, we first discuss the characteristics of a nanopore under different electrical biases applied to a single layer 23 nm thick n−Si membrane and their effects on the ionic current−voltage characteristics.

Figure 2 illustrates the potential variations along the nanopore axis for several membrane biases and the corresponding current−voltage characteristics ($I-V$ curves) and flux curves for the cylindrical (Figure 2A−C) and conical (Figure 2D−F) nanopore geometries. As the membrane layer bias varies from −1 to 1 V, the electrostatic potential profile in the nanopore changes from a potential well to a potential barrier (Figure 2A,D), as the result of the combined effect of several sources of charge in the membrane, such as dopant charges, membrane charge σ, and electron−hole charge.[18,26] The current voltage characteristics for a cylindrical nanopore with a single layer membrane is ohmic (Figure 2B), with the conductance depending on the total charge accumulated in the nanopore. However, one notices that irrespectively of whether the potential profile in the nanopore is a barrier or a well the $I-V$ curves for $V_n = -1$ and 0.5 V or −0.5 and 0 V almost coincide. Even though these $I-V$ curves are almost identical, the contributions from the K^+ and Cl^- fluxes are different as seen in Figure 2C, which shows specifically

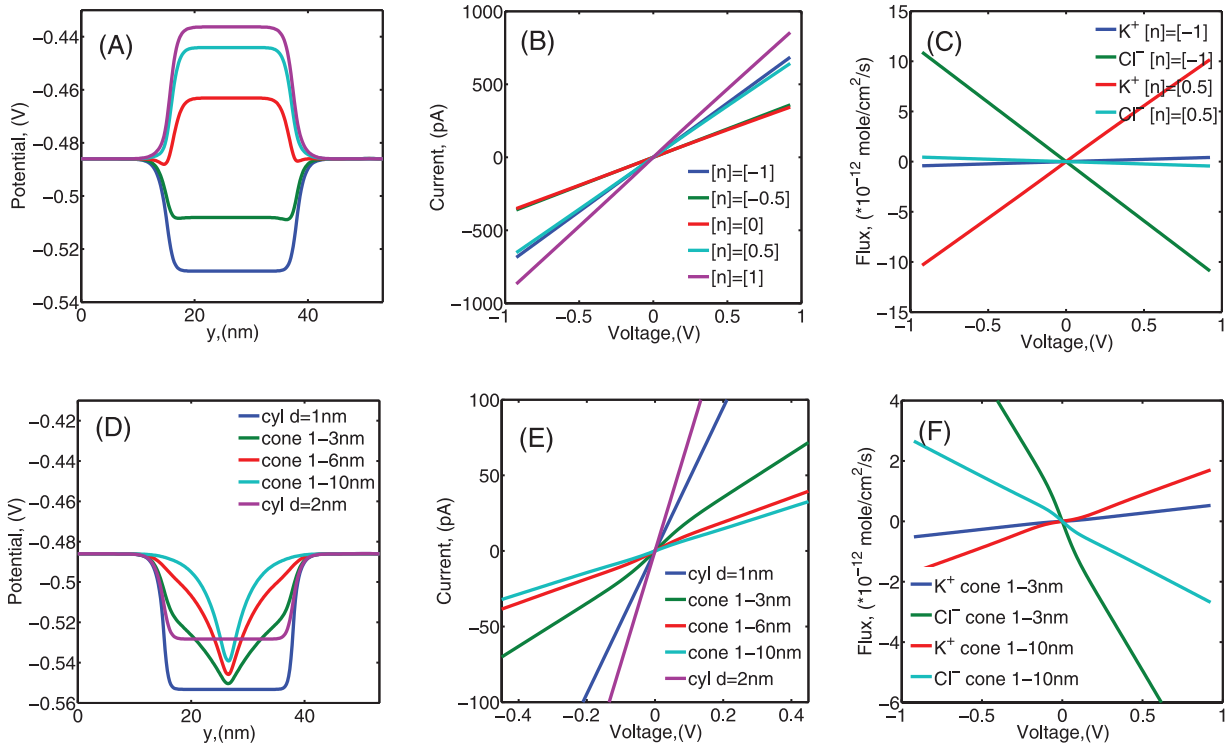

Figure 2. Single layer n-type semiconductor membrane (the solution concentration is 0.1 M) with cylindrical (A−C) and conical (D−F) nanopores with different opening diameters at the membrane surface (see legend, $V_n = -1$ V): (A and D) Electrostatic potential along the axis through the center of the nanopore; (B and E) *I*−*V* curves for potential profiles in (A); (C and F) ionic fluxes through the nanopore.

the ionic fluxes for $V_n = -1$ and 0.5 V. It can be seen that the total current flowing through the nanopore in the former case is carried mostly by Cl^- ions, whereas main contribution to the current in the latter case comes from K^+ flux. This is due to the fact that the two types of ions have opposite charge and the same mobility, and the potential barrier for cations is a potential well for anions, and *vice versa*. Thus, a single layer cylindrical membrane can operate as an ion filter, which, depending on the membrane bias, lets through ions of one charge and blocks the flow of the oppositely charged ion species.

The conical geometry of the nanopore results in an effective decrease of the membrane thickness manifested in smaller overall extensions of the membrane potential well as shown in Figure 2D, while the narrower nanopore in the center of the membrane (1 nm) results in a larger value of the potential in this region compared to the 2 nm cylindrical nanopore case (Figure 2A).

Figure 2E shows that the *I*−*V* characteristics of conical pores exhibit a larger conductance at low bias (switching) than at high bias, mostly visible in the 1−3 nm conic pore (dark green curve). Unlike the *I*−*V* characteristics of cylindrical pores, which are ohmic for the whole bias range (for the chosen membrane parameters). In a conical pore, this conductance variation is due to the shape of the nanopore, which induces a large potential as well as carrier density variation (Figure 2B).

Within our transport model, we find that low electrolyte bias cannot "shift" K^+ ions accumulated in the nanopore (large K^+ concentration), while a larger bias pulls them from that region, leading to a saturation-like slow increase in the flux with applied bias (decreased ionic concentration in the nanopore; Figure 2E,F). In this voltage interval, Cl^- flux is small as there is no substantial presence of these ions in the nanopore. At even higher biases, only drift term in the current density survives, which eventually leads to a linear (ohmic) *I*−*V* dependence. This is reminiscent of the triple layered membrane (see below) where two n−p diodes are connected in reverse, resulting in the transistor-like *I*−*V* curves with a switching region (abrupt, step-like increase in the current) at small solution biases.

We should emphasize here that the nascent transistor-like behavior of the current is very sensitive to the geometry of the pore as well as to the charge distribution on the surface and inside the membrane. For example, as can be seen in Figure 2E,F, the switching region is not observable for the cylindrical pores and greatly diminished for the conical pores with very large membrane openings because of the smaller central barrier/well for these nanopore geometries.

Double Layer Membrane: Ionic Rectifier. Next, we briefly consider a double (np) layer semiconductor membrane with a cylindrical 2 nm nanopore. Figure 3 dis-

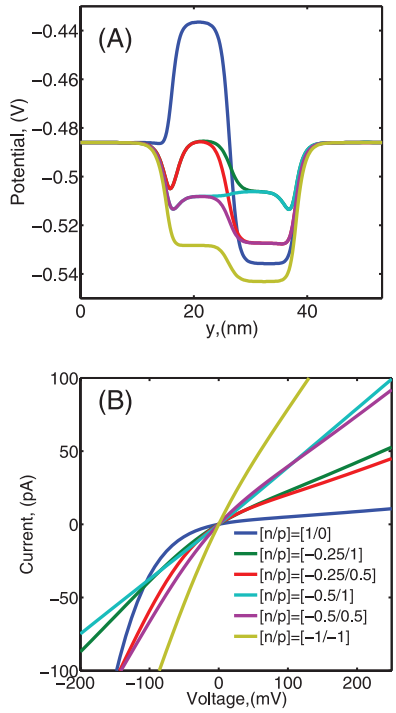

Figure 3. Same as in Figure 2A,B, but for the double layer np semiconductor membrane.

plays the potential variation along the nanopore axis for several membrane biases (Figure 3A) and the corresponding $I-V$ curves (Figure 3B). Unlike the electrostatic potential profile produced by the single layer n−Si membrane (Figure 2A) that exhibits a single potential extremum (which can be either positive or negative) for all considered membrane biases, the potential along the channel in a np-membrane produces either a single dominant minimum or two extrema (one minimum and one maximum) as a function of applied bias between the n- and p-layers (Figure 3A). This feature of the np-membrane to produce asymmetric potential profile in the channel is the direct cause for ionic current rectification properties of the double layered nanopore membranes. Thus, the maximum current rectification is obtained for membrane biases n−Si at $V_n = 1$ V and p−Si at $V_p = 0$ V (see Figure 3B), for which there is a maximal potential variation.

Let us point out that typical potential variations in the pore are $\gtrsim$50 mV (Figure 3A) and are larger than the thermal voltage $kT/e \simeq 25$ mV; we obtain larger potential variations at lower ion concentrations [KCl] $<$ 0.1M due to reduced screening of the nanopore walls by ions and, consequently, improved selectivity and rectification function. The complete discussion of the np-membrane system can be found in ref 27.

Triple Layer Membrane: Current Blocking and Switching. Finally, we consider semiconductor membrane with three (npn) layers (Figure 1). Electrostatic potential variations through the nanopore center for different membrane biases are shown in Figure 4A,C,E, while the corresponding current−voltage characteristics are presented in Figure 4B,D,F.

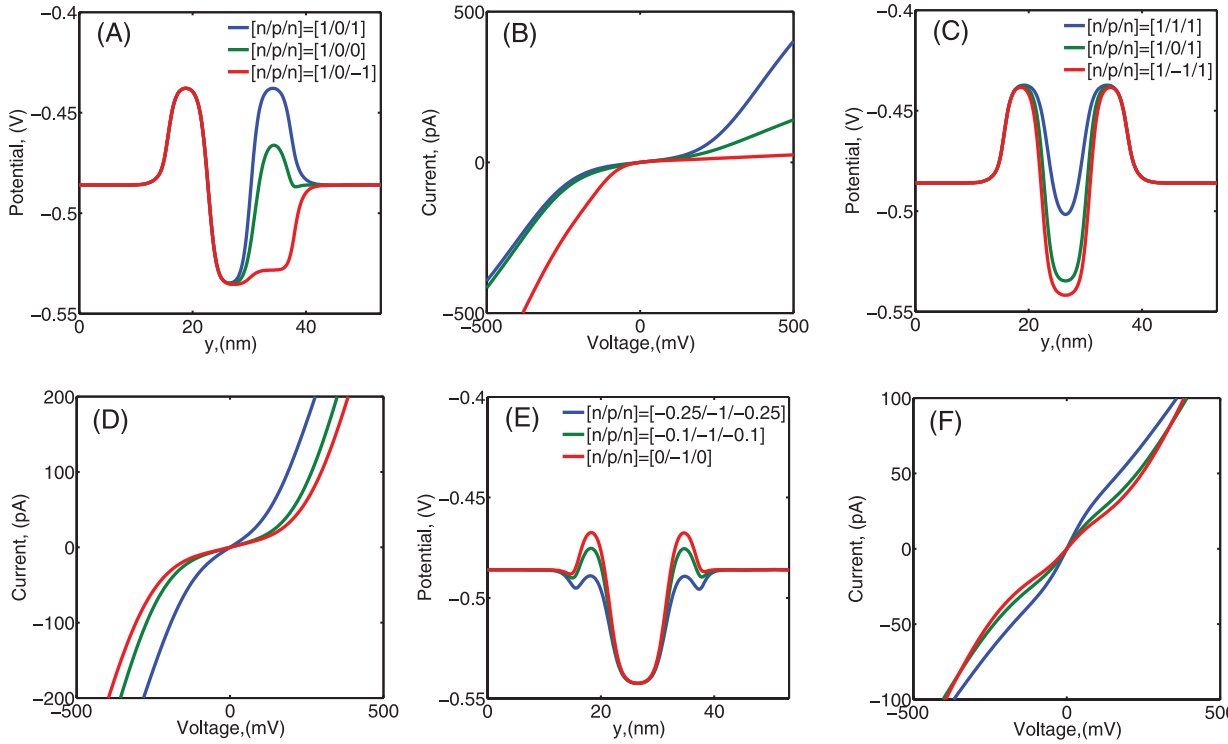

Figure 4. Triple layer npn semiconductor membrane (solution concentration is 0.1 M): (A,B) electrostatic potential along the nanopore axis and corresponding $I-V$ curves for varying bias on the lower n−Si layer: $[V_{n(top)}/V_p/V_{n(bottom)}] = [1/0/1]$, [1/0/0], and [1/0/−1]; (C,D) the same for varying bias on the p−Si middle layer: [1/1/1], [1/0/1], and [1/−1/1]; (E,F) the same for varying bias on the bottom and the top n−Si layers in sync: [−0.25/−1/−0.25], [−0.1/−1/−0.1], and [0/−1/0].

We first vary the membrane bias at the bottom n−Si layer between −1 and 1 V, keeping the biases at the top n−Si and the middle p−Si layer constant at V_n = 1 V (top layer) and V_p = 0 V, respectively (Figure 4A). The electrostatic potential in the nanopore evolves from the three extrema profile (as in double-humped camel) for membrane layer biases [$V_{n(top)}/V_p/V_{n(bottom)}$] = [1 V/0 V/1 V] (short notation: [n/p/n] = [1/0/1]) to the asymmetric profile with two extrema for [n/p/n] = [1/0/−1], which is qualitatively similar to the results for the np double layered membrane at [n/p] = [1/0] (Figure 3A). In this case, the current−voltage characteristics (Figure 4B) becomes diode-like, that is, rectifying, for [n/p/n] = [1/0/−1], while for membrane layer biases [n/p/n] = [1/0/1] and [n/p/n] = [1/0/0], they result in bidirectional current blocking over the voltage window ∼−50 to +150 mV. At larger electrolyte voltages, the current through the nanopore grows linearly. The current slope for positive voltages changes with applied membrane bias until the *I*−*V* curve becomes flat, which corresponds to full current rectification (red curve). The direction of the current blockade can be inverted if membrane layer biases are changed from [n/p/n] = [1/0/−1] to [n/p/n] = [−1/0/1]. Thus, the triple layered structure allows control over the ionic flow in both directions without membrane treatment, electrolyte pH adjustment, *etc*.

Hence, the potential at the top and bottom n−Si layers in the triple layered membrane controls the transition of the *I*−*V* curves from either bidirectional blocking or switching to a diode-like behavior obtained with the double layered membrane. Also, the electrical potential in the nanopore can be further adjusted to form a single extremum similar to that of a single layer membrane (not shown).

In Figure 4C, we show the effect of the membrane layer bias on the middle p−Si layer (biases at the top and the bottom n−Si layers are fixed at V_n = 1 V) on the *I*−*V* characteristics. The depth of the potential in the middle layer regulates the extent of the bidirectional current blocking (Figure 4D), where one can see that deeper potentials in the membrane middle layer result in a wider voltage window of current blocking.

Finally, as illustrated in Figure 4E,F, the transition from current "blocking" to "switching", that is, onset of a step-like current increase in the *I*−*V* curves around *V* ∼ 0, is regulated by simultaneously lowering the height of the potential barriers at the top and bottom layers of the membrane, while keeping the bias at the middle layer constant, thereby making the triple layer membrane potential behave in a similar way to the single layer membrane analyzed before (Figure 2). This effect is magnified for smaller diameter pores as shown in Figure 5 for a 1 nm diameter cylindrical pore. Note that the switching behavior is more pronounced in triple than in the single layer membranes (Figure 2E) because of the thin central p-doped region responsible for dominant potential well (7 *vs* 21 nm thick single layer membrane).

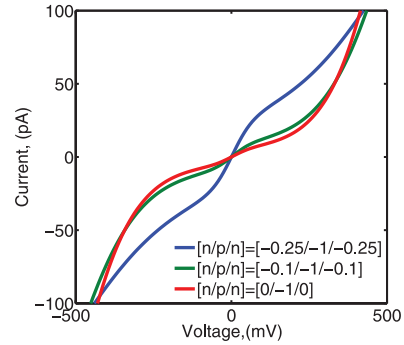

Figure 5. Triple layer npn semiconductor membrane: current−voltage characteristics for three membrane biases (see legend) for a 1 nm diameter cylinder nanopore and electrolyte concentration 0.1 M.

In Figure 6, the *I*−*V* curves computed for different solution concentrations in the case of the triple layered membrane under bias [n/p/n] = [−0.25/−1/−0.25] are shown. One can see that, as expected, the conductance increases with the solution concentration. The magnitude of the "step" in the *I*−*V* curves near *V* ∼ 0 first increases with the electrolyte concentration, but eventually smoothes over to a linear dependence as the larger concentration effectively screens out the membrane-induced potential. This behavior is similar to recent experimental observations.[22] The relative size of the steps depends on the depth of the potential in the membrane middle layer: The deeper this well, the larger the step in the *I*−*V* curve. Lower electrolyte concentrations lead to reduced membrane screening and to a larger influence of the membrane bias on the ion current. Thus, the switching region in the current is more pronounced for 0.01 M electrolyte concentration.

CONCLUSIONS

Doped semiconductor membranes are of particular interest in nanofluidics due to their electrical tunability. In this work, we focused on the electrical properties of nanopores in doped Si membranes consisting of

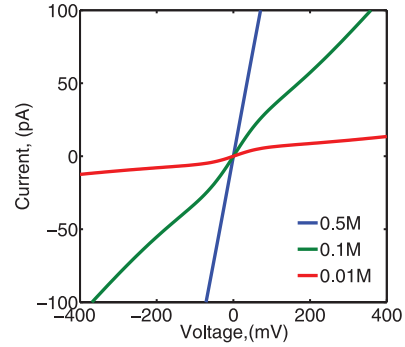

Figure 6. Triple layer npn semiconductor membrane: current−voltage characteristics for bias [n/p/n] = [−0.25/−1/−0.25] for a 2 nm diameter cylinder nanopore and different electrolyte concentrations.

single n, double np, and triple npn layers. It was shown[18] that single layer membranes can function as ionic filters but also exhibit an additional regime of current switching which is caused by the shape of the electrical potential in the nanopore. This regime was not reported in our work previously. While, double layered membranes can be biased to perform ion current rectification,[27] the addition of the third layer allows one to broaden the device functions to include such regimes as bidirectional current blocking and current switching, while retaining such regimes as current filtering and rectification at certain membrane biases. It is expected that future applications of these membranes might include ionic current control, biomolecule separation, and DNA nanofluidic systems. Multilayered membranes can be used to provide much needed control over the DNA translocation through a nanopore, for example, to slow down DNA translocation and facilitate back-and-forth as well as stop-and-go DNA translocation to increase molecule sampling time in the nanopore.

METHODS

To obtain the ion charge distribution in the nanopore, the Poisson equation is solved self-consistently by a multigrid method in the electrolyte−membrane system,[8] assuming the ions in the electrolyte are fully dissociated and obey the Boltzmann distribution, whereas electrons and holes in the semiconductor are governed by the Fermi−Dirac statistics. The model details are described elsewhere.[8,27] We use virtual solid-state parameters for the solution, which enables us to formulate an all-semiconductor model for the charge and electric potential in the electrolyte and solid-state materials.[30]

We model the bias potentials applied to the membrane layers with respect to the electrolyte by varying the quasi-Fermi levels of the Si n- (V_n) and p (V_p)-layers of the membrane separately over the −1 to 1 V range; we refer to these as "membrane layer biases" further on. Note that they should be distinguished from the "electrolyte bias" V that is applied between the top and the bottom electrolyte chamber located above and below the membrane (see Figure 1).

Acknowledgment. This work was funded by NIH Grant ROI-HG003713-01. The authors gratefully acknowledge the use of the supercomputer time at the National Center for Supercomputer Applications.

REFERENCES AND NOTES

1. Alberts, B.; Bray, D.; Johnson, A.; Lewis, J.; Raff, M.; Roberts, K.; Walter, P. *Essential Cell Biology*; Garland Science/Taylor and Francis Group: New York, 2003.
2. Beckstein, O.; Sansom, M. The Influence of Geometry, Surface Character, and Flexibility on the Permeation of Ions and Water through Biological Pores. *Phys. Biol.* **2004**, *1*, 42–52.
3. Korchev, Y. E.; Bashford, C. L.; Alder, G. M.; Apel, P. Y.; Edmonds, D. T.; Lev, A. A.; Nandi, K.; Zima, A. V.; Pasternak, C. A. A Novel Explanation for Fluctuations of Ion Current through Narrow Pores. *FASEB J.* **1997**, *11*, 600–608.
4. Lev, A. A.; Korchev, Y. E.; Rostovtseva, T. K.; Bashford, C. L.; Edmonds, D. T.; Pasternak, C. A. Rapid Switching of Ion Current in Narrow Pores: Implications for Biological Ion Channels. *Proc. Biol. Sci.* **1993**, *252*, 187–192.
5. Bashford, C. L.; Alder, G. M.; Pasternak, C. A. Fluctuation of Surface Charge in Membrane Pores. *Biophys. J.* **2004**, *82*, 2032–2040.
6. Li, J.; Stein, D.; McMullan, C.; Branton, D.; Aziz, M. J.; Golovchenko, J. A. Ion-Beam Sculpting at Nanometre Length Scales. *Nature* **2001**, *412*, 166–169.
7. Storm, A. J.; Chen, J. H.; Ling, X. S.; Zandbergen, H. W.; Dekker, C. Fabrication of Solid-State Nanopores with Single-Nanometre Precision. *Nat. Mater.* **2003**, *2*, 537–540.
8. Gracheva, M. E.; Xiong, A.; Aksimentiev, A.; Schulten, K.; Timp, G.; Leburton, J.-P. Simulation of the Electric Response of DNA Translocation through a Semiconductor Nanopore-Capacitor. *Nanotechnology* **2006**, *17*, 622–633.
9. Heng, J. B.; Ho, C.; Kim, T.; Timp, R.; Aksimentiev, A.; Grinkova, Y. V.; Sligar, S.; Schulten, K.; Timp, G. Sizing DNA Using a Nanometer-Diameter Pore. *Biophys. J.* **2004**, *87*, 2905–2911.
10. Kasianowicz, J. J.; Brandin, E.; Branton, D.; Deamer, D. W. Characterization of Individual Polynucleotide Molecules Using a Membrane Channel. *Proc. Natl. Acad. Sci. U.S.A.* **1996**, *93*, 13770–13773.
11. Vlassiouk, I.; Siwy, Z. Nanofluidic Diode. *Nano Lett.* **2007**, *7*, 552–556.
12. Karnik, R.; Duan, C.; Castelino, K.; Daiguji, H.; Majumdar, A. Rectification of Ionic Current in a Nanofluidic Diode. *Nano Lett.* **2007**, *7*, 547–551.
13. Siwy, Z.; Heins, E.; Harrell, C.; Kohli, P.; Martin, C. Conical-Nanotube Ion-Current Rectifiers: The Role of Surface Charge. *J. Am. Chem. Soc.* **2004**, *126*, 10850–10851.
14. Siwy, Z. Ion Current Rectification in Nanopores and Nanotubes with Broken Symmetry Revisited. *Adv. Funct. Mater.* **2006**, *16*, 735–746.
15. Cervera, J.; Schiedt, B.; Neumann, R.; Mafé, S.; Ramírez, P. Ionic Conduction, Rectification, and Selectivity in Single Conical Nanopores. *J. Chem. Phys.* **2006**, *124*, 104706–104715.
16. Horiuchi, P.; Dutta, P. Electrokinetic Flow Control in Microfluidic Chip Using A Field-Effect Transistor. *Lab Chip* **2006**, *6*, 714–723.
17. Daiguji, H.; Oka, Y.; Shirono, K. Nanofluidic Diode and Bipolar Transistor. *Nano Lett.* **2005**, *5*, 2274–2280.
18. Vidal, J.; Gracheva, M. E.; Leburton, J.-P. Electrically Tunable Solid-State Silicon Nanopore Ion Filter. *Nanoscale Res. Lett.* **2007**, *2*, 61–68.
19. Ho, C.; Qiao, R.; Heng, J. B.; Chatterjee, A.; Timp, R. J.; Aluru, N. R.; Timp, G. Electrolytic Transport Through a Synthetic Nanometer-Diameter Pore. *Proc. Natl. Acad. Sci. U.S.A.* **2005**, *102*, 10445–10450.
20. Fologea, D.; Uplinger, J.; Thomas, B.; McNabb, D. S.; Li, J. Slowing DNA Translocation in a Solid-State Nanopore. *Nano Lett.* **2005**, *5*, 1734–1737.
21. Fan, R.; Karnik, R.; Yue, M.; Li, D.; Majumdar, A.; Yang, P. DNA Translocation in Inorganic Nanotubes. *Nano Lett.* **2005**, *5*, 1633–1637.
22. Kalman, E.; Vlassiouk, I.; Siwy, Z. S. Nanofluidic Bipolar Transistor. *Adv. Mater.* **2008**, *20*, 293–297.
23. Nishizawa, M.; Menon, V. P.; Martin, C. R. Metal Nanotubule Membranes with Electrochemically Switchable Ion-Transport Selectivity. *Science* **1995**, *268*, 700–702.
24. Karnik, R.; Fan, R.; Yue, M.; Li, D.; Yang, P.; Majumdar, A. Electrostatic Control of Ions and Molecules in Nanofluidic Transistors. *Nano Lett.* **2005**, *5*, 943–948.
25. Dimitrov, V.; Aksimentiev, A.; Schulten, K.; Heng, J.; Sorsch, T.; Mansfield, W.; Miner, J.; Watson, G. P.; Cirelli, R.; Klemens, F. Exploring the Prospects for a Nanometer-Scale Gene Chip. *IEDM Tech. Digest* **2006**, 169–173.
26. Gracheva, M. E.; Leburton, J.-P. Electrolytic Charge Inversion at the Liquid−Solid Interface in a Nanopore in a Doped Semiconductor Membrane. *Nanotechnology* **2007**, *18*, 145704–145710.
27. Gracheva, M. E.; Vidal, J.; Leburton, J.-P. p-n Semiconductor Membrane for Electrically Tunable Ion Current Rectification and Filtering. *Nano Lett.* **2007**, *7*, 1717–1722.
28. Lakshminarayanaiah, N. *Equations of Membrane Biophysics*; Academic: New York, 1984.

29. Ramírez, P.; Mafé, S.; Aguilella, V. M.; Alcaraz, A. Synthetic Nanopores with Fixed Charges: An Electrodiffusion Model for Ionic Transport. *Phys. Rev. E* **2003**, *68*, 011910(1)011910(8) .
30. Gardner, C. L.; Nonner, W.; Eisenberg, R. S. Electrodiffusion Model Simulation of Ionic Channels: 1D Simulations. *J. Comp. Elect.* **2004**, *3*, 25–31.